

PEAK ENERGY CLUSTERING AND EFFICIENCY IN COMPACT OBJECTS

ASAF PE'ER^{1,2,3}, PETER MÉSZÁROS² AND MARTIN J. REES⁴

Draft version September 9, 2018

ABSTRACT

We study the properties of plasmas containing a low energy thermal photon component at comoving temperature $\theta \equiv kT'/m_e c^2 \sim 10^{-5} - 10^{-2}$ interacting with an energetic electron component, characteristic of, e.g., the dissipation phase of relativistic outflows in gamma-ray bursts (GRB's), X-ray flashes, and blazars. We show that, for scattering optical depths larger than a few, balance between Compton and inverse-Compton scattering leads to the accumulation of electrons at values of $\gamma\beta \sim 0.1 - 0.3$. For optical depths larger than ~ 100 , this leads to a peak in the comoving photon spectrum at $1 - 10$ keV, very weakly dependent on the values of the free parameters. In particular, these results are applicable to the internal shock model of GRB, as well as to slow dissipation models, e.g. as might be expected from reconnection, if the dissipation occurs at a sub-photospheric radii. For GRB bulk Lorentz factors ~ 100 , this results in observed spectral peaks clustering in the $0.1 - 1$ MeV range, with conversion efficiencies of electron into photon energy in the BATSE range of $\sim 30\%$.

Subject headings: gamma rays: bursts — gamma rays: theory — plasmas — radiation mechanisms: non-thermal

1. INTRODUCTION

The widely accepted interpretation of gamma-ray burst (GRB) phenomenology is that the observable radiation is due to the dissipation of the kinetic energy of a relativistic outflow, powered by a central compact object (for reviews, see, e.g., Mészáros 2002; Waxman 2003; Piran 2004). The dissipated energy is assumed to be converted to energetic electrons, which produce high energy photons by synchrotron radiation and inverse Compton (IC) scattering. Similar considerations are assumed to apply to X-ray flashes (XRFs) and some models of blazars (e.g., Guetta *et al.* 2004).

Even though the optically thin synchrotron-IC emission model of GRB's (Band *et al.* 1993; Tavani 1996; Preece *et al.* 1998) and blazars is in general agreement with observations, two concerns are often raised in particular for GRBs. The γ -ray break energy of most GRB's observed by BATSE is in the range 100 keV - 300 keV (Brainerd 1998; Preece *et al.* 2000). It is thought that clustering of the peak emission in this narrow energy range requires fine tuning of the fireball model parameters. In addition, there is evidence in some bursts for low-energy spectral slopes steeper than the optically thin synchrotron predictions (Crider *et al.* 1997; Preece *et al.* 1998; Frontera *et al.* 2000; Ghirlanda *et al.* 2003).

This has led several authors to consider alternative scenarios for the γ -ray emission, such as Compton drag (Lazzati *et al.* 2000), or the contribution of a photospheric term (Mészáros & Rees 2000; Mészáros *et al.* 2002; Rees & Mészáros 2004) (but see also Stern & Poutanen 2004). In the “photospheric” model, thermal radiation, originating near the base of the flow emerges from a “photospheric radius” at

which the flow becomes optically thin. As shown in Rees & Mészáros (2004), dissipation processes can occur at radii smaller than the photosphere radius, increasing the energy available to produce thermal seed photons which can be IC scattered by relativistic electrons. The high optical depth to scattering by the electrons (and the created pairs) results in a spectrum that is significantly different than the optically thin synchrotron-SSC model predictions.

The spectrum from internal collisions at a high scattering optical depth was studied by Pe'er & Waxman (2004), with a numerical model which calculates self-consistently the photon and electron distributions (Pe'er & Waxman 2004b). Although a thermal component was not considered in this work, it was found that a large number of pairs can be created, and for optical depths $\tau_{\pm} \sim 100$, the emission peaks at ~ 1 MeV. This result was found to be very robust, with a very weak dependence on the values of the free parameters.

In this letter, we analyze numerically and analytically the emission resulting from the interaction of energetic electrons with a low energy thermal photon component, under conditions of intermediate to large scattering optical depths, $\tau \approx 10 - 100$. We show in §2 that the relativistic electrons lose their energy and accumulate around (comoving) momentum values $\gamma\beta \approx 0.1 - 0.3$. This results from a balance between inverse-Compton cooling and Compton heating, which is very insensitive to other input parameters. For a bulk Lorentz factor $\Gamma \sim 10^2$ as observed in GRB (or $\Gamma \sim 10 - 50$ in blazars) an observed Wien peak at $\lesssim 1$ MeV is thus obtained. In §3 we specify a model for the GRB prompt emission, in which part of the dissipation or internal collisions occur near or below the photospheric radius. We show in §4 that using the commonly assumed values of the free parameters of the fireball model, a spectral peak at $\lesssim 1$ MeV is obtained, with a radiative efficiency which can be substantially higher than for standard internal shocks. We also consider a “slow dissipation” case, which might characterize magnetic dissipation models, where electrons are

¹ Astronomical Institute “Anton Pannekoek”, Kruislaan 403, 1098SJ Amsterdam, the Netherlands

² Dpt. Astron. & Astrophysics, Dpt. Physics, Pennsylvania State University, University Park, PA 16802

³ apeer@science.uva.nl

⁴ Institute of Astronomy, University of Cambridge, Madingley Rd., Cambridge CB3 0HA, UK

reenergized to lower energies multiple times, leading to a similar peak energy clustering and efficiency. We discuss in §5 the implications for GRB, XRF and AGN.

2. ELECTRON ENERGY BALANCE

We consider a plasma cloud of characteristic comoving length Δ , containing a thermal component of low energy photons at a normalized comoving temperature $\theta \equiv kT'/m_e c^2$, with an external source (e.g., shocks or other dissipative processes) which continuously injects into the plasma isotropically distributed electrons at a characteristic Lorentz factor γ_m , at a constant rate during the comoving dynamical time $t_{dyn} \equiv \Delta/c$. The initial energy density of the photon component, u_{ph} , is parametrized relative to the injected electron energy density u_{el} through the numerical factor $A = u_{ph}/u_{el}$. For models of GRBs and XRFs, if the dissipative process occurs near or below the Thompson photosphere, a typical value is $A \sim 1$ (see equ. 15). For $A > \theta/\gamma_m \sim 10^{-4}$, the occupation number of up-scattered photons is much smaller than unity, and induced scattering can be ignored. We assume (I) that $\gamma_m \theta < 1$, i.e. that the scattering is in the Thompson regime; and (II) that $\gamma_m^2 \theta > 1$, i.e., that electrons scatter photons to energies above the electron's rest mass energy.

If the main electron energy loss is inverse-Compton scattering, the injected electrons lose energy at an initial rate $\dot{t}_{loss} = \gamma_m m_e c^2 / (4/3) c \sigma_T \gamma_m^2 u_{ph}$, and cool down to $\gamma_f \simeq 1$ on a total loss time $t_{loss} = \dot{t}_{loss} \times \gamma_m$, therefore

$$\frac{t_{loss}}{t_{dyn}} = \frac{3}{4c\sigma_T A n_{el} \gamma_m t_{dyn}} = \frac{3}{4A\gamma_m \tau_{\gamma_e}}. \quad (1)$$

Here $n_{el} = u_{el}/\gamma_m m_e c^2$, and τ_{γ_e} is the electron scattering optical depth. Thus, for $\tau_{\gamma_e} > 1$, electrons accumulate at $\gamma_f \approx 1$ on a time shorter than the dynamical time.

For concreteness we focus below on the internal shock case (the qualitatively similar slow dissipation case is discussed in more detail in Pe'er *et al.* 2005). The cooled electrons form a steady state power law distribution in the range $\gamma_f < \gamma < \gamma_m$, of the form $n_{el}(\gamma\beta) \propto (\gamma\beta)^{-2}$, where $\beta = (1 - \gamma^{-2})^{1/2}$. The emitted photon spectrum in the range $3\theta m_e c^2 < \varepsilon < 4\theta \gamma_m^2 m_e c^2$ is $n_\gamma(\varepsilon) \propto \varepsilon^{-3/2}$, thus the characteristic energy of photons more energetic than $m_e c^2$ is not far above $m_e c^2$. These photons receive nearly all of the energy of the injected electrons.

The value of the electron momenta at the end of the dynamical time, $\gamma_f \beta_f$, can now be calculated as a function of the optical depth, the initial photon temperature θ , and the ratio of energies A . This value is estimated by balance between energy loss due to inverse-Compton scattering of soft photons at energies $\varepsilon < m_e c^2$, and energy gain by direct Compton scattering photons more energetic than $m_e c^2$. As we show below, the weak dependence of $\gamma_f \beta_f$ on any of the values of the free parameters is a key result that implies weak dependence of the observed spectral peak on the values of the free parameters, for intermediate to high values of the optical depth.

A photon with energy $\varepsilon > m_e c^2$, undergoing Compton scattering with an isotropically distributed electron density n_{el} with sub-relativistic velocity $\gamma \simeq 1$, loses energy

at a constant rate^{5 6}

$$\frac{d\varepsilon}{dt} \simeq -c\sigma_T(m_e c^2/2)n_{el}. \quad (2)$$

This result is valid for photon energies $\gtrsim f m_e c^2$, where $f \simeq 3$. The injection rate by IC scattering of photons at energies $\gtrsim f m_e c^2$ is approximated by $dn_{ph}(\varepsilon > f m_e c^2)/dt \approx u_{el}/f m_e c^2 t_{dyn}$. These photons lose energy by down-scattering to energies below $f m_e c^2$ on a time scale $\varepsilon/(d\varepsilon/dt) = 2ft_{dyn}/\tau_{\gamma_e}$, which is shorter than the dynamical time for $\tau_{\gamma_e} > 2f \simeq 6$. Assuming $\tau_{\gamma_e} > few$, the photon's number density approaches a steady value given by

$$n_{ph}(\varepsilon \gtrsim f m_e c^2) \approx \frac{u_{el}}{m_e c^2} \frac{2}{\tau_{\gamma_e}}. \quad (3)$$

The rate of energy gain by an electron at γ_f due to Compton scattering of these photons is therefore

$$\frac{dE_+}{dt} \approx \frac{m_e c^2}{2} c\sigma_T \frac{2u_{el}}{m_e c^2 \tau_{\gamma_e}}. \quad (4)$$

In the Thompson regime, which is valid for photons at energies $\varepsilon(n_{sc}) \lesssim (\gamma_f \beta_f)^2 m_e c^2 / f$ with $f \approx 3$, electrons at γ_f up-scatter the low energy thermal photons at a rate $\approx n_{ph} c \sigma_T$, where $n_{ph} \approx u_{ph}/3\theta m_e c^2$. In this regime, the increase in the photon energy at each scattering is $\Delta\varepsilon = (4/3)(\gamma_f \beta_f)^2 \varepsilon(n_{sc})$, and the photon energy after n_{sc} scattering is $\varepsilon(n_{sc}) \approx 3\theta m_e c^2 \exp(4/3(\gamma_f \beta_f)^2 n_{sc})$ where $\beta_f \equiv (1 - \gamma_f^{-2})^{1/2}$. For $\tau_{\gamma_e} > few$, nearly all of the photons are being scattered and do not leave the plasma during the dynamical time, therefore the electron energy loss rate is time independent, given by

$$\frac{dE_-}{dt} \approx (4/3)(\gamma_f \beta_f)^2 c\sigma_T u_{ph} e^{4/3(\gamma_f \beta_f)^2 n_{sc}}. \quad (5)$$

Equating the energy loss and energy gain rates,

$$(\gamma_f \beta_f)^2 e^{4/3(\gamma_f \beta_f)^2 n_{sc}} = \frac{3}{4A\tau_{\gamma_e}}. \quad (6)$$

For optical depths not much larger than a few, the exponent on the right hand side of equation 6 can be approximated as 1, since for a relativistically expanding plasma $\tau_{\gamma_e} \simeq n_{sc}$, and $\gamma_f \beta_f < 1$. In this approximation, the steady state electron momentum is given by

$$\gamma_f \beta_f (n_{sc} \lesssim 10) \approx \left(\frac{3}{4A\tau_{\gamma_e}} \right)^{1/2} \approx 0.3 A_0^{-1/2} \tau_{\gamma_e,1}^{-1/2}, \quad (7)$$

where $\tau_{\gamma_e} = 10^1 \tau_{\gamma_e,1}$ assumed. The spectral peak after an intermediate number of scatterings is thus expected between $\theta m_e c^2$ and $(\gamma_f \beta_f)^2 m_e c^2$.

For optical depths larger than a few tens, low energy photons can be upscattered to a maximum energy $(\gamma_f \beta_f)^2 m_e c^2 / f$ in the Thompson regime, and the exponent in equation 6 is approximated by $\exp(4/3(\gamma_f \beta_f)^2 n_{sc}) \approx (\gamma_f \beta_f)^2 / 3\theta f$. The steady state electron momentum is therefore

$$\gamma_f \beta_f \approx \left(\frac{9\theta f}{4A\tau_{\gamma_e}} \right)^{1/4} \approx 0.1 \theta_{-3}^{1/4} A_0^{-1/4} \tau_{\gamma_e,2}^{-1/4}, \quad (8)$$

⁵ See <http://staff.science.uva.nl/~apeer>; A derivative of this result also appears in Pe'er *et al.* (2005).

⁶ Roughly, Klein-Nishina Compton cross section is $\sigma(\varepsilon) \approx (3/16)\sigma_T \times m_e c^2 \varepsilon^{-1}$, thus $d\varepsilon/dt \approx c\sigma_T n_{el} m_e c^2 \varepsilon^0$. Full analytical treatment gives the numerical pre-factor 1/2.

where $\theta = 10^{-3}\theta_{-3}$, $A = 10^0 A_0$, and $\tau_{\gamma e} = 10^2 \tau_{\gamma e,2}$ were assumed. The number of scatterings required for photons to be upscattered to $(\gamma_f \beta_f)^2 m_e c^2 / f$ can be estimated as

$$n_{sc} \approx \frac{\log\left(\frac{(\gamma_f \beta_f)^2}{3\theta f}\right)}{\frac{4}{3}(\gamma_f \beta_f)^2} \approx 10^{1.5} - 10^{2.5}, \quad (9)$$

for θ in the range $10^{-5} - 10^{-2}$. For this number of scatterings, the spectral peak is expected at $(\gamma_f \beta_f)^2 m_e c^2 / f \simeq 1 - 3$ keV (in the plasma frame). Both this result and the result in eq. 8 show a very weak dependence on any of the parameter values.

For optical depths higher than the values given in eq. 9, photons are upscattered to energies above $(\gamma_f \beta_f)^2 m_e c^2 / f$ outside the Thompson regime. The final photon energy is therefore limited to a narrow range, $(\gamma_f \beta_f)^2 m_e c^2 / f \leq \varepsilon(n_{sc}) \leq (\gamma_f \beta_f)^2 m_e c^2$, and a Wien peak is formed. Since the average photon energy is equal to the average kinetic energy of the electron in this case, a Compton equilibrium is formed (Guilbert *et al.* 1983; Lightman & Zdziarski 1987; Svensson 1987), the final electron momentum is

$$\gamma_f \beta_f = [3\theta(1 + A^{-1})]^{1/2} = 0.08 \theta_{-3}^{1/2}, \quad (10)$$

and a Wien peak is formed at

$$\varepsilon_{WP} \approx 3\theta m_e c^2 \times (1 + A^{-1}) \simeq 10 \text{ keV}, \quad (11)$$

irrespective of the value of the optical depth.

Pairs produced by $\gamma\gamma$ will accumulate at $\gamma_f \beta_f$, while lowering of the number density of energetic photons, hence lowering the value of $\gamma_f \beta_f$. We estimate the significance of this effect using the pair production rate of photons at energy ε , $dt(\varepsilon)^{-1} \approx (1/4)c\sigma_T n_{ph}(\tilde{\varepsilon} \gtrsim (m_e c^2)^2 / \varepsilon)$. The ratio of the characteristic times for pair production and Compton scattering by electrons at $\gamma_f \simeq 1$, for photons at energy $f m_e c^2$ is

$$\frac{t_{loss}|_{p,p}}{t_{loss}|_C} \simeq \frac{n_{el}}{f n_{ph} \left(\tilde{\varepsilon} \gtrsim \frac{m_e c^2}{f}\right)}. \quad (12)$$

If Compton scattering is the only mechanism producing photons above the thermal peak, then $n_{ph}(\tilde{\varepsilon} \gtrsim m_e c^2 / f) \approx n_{el} \times (f/\theta)^{1/2}$. In this case, the number density of photons at $\gtrsim f m_e c^2$ is given by equation 3, corrected by a factor $2\theta^{1/2} f^{-3/2} = 3.8 \times 10^{-2} \theta_{-2}^{1/2} f_{0.5}^{-3/2}$, where $f = 10^{0.5} f_{0.5}$. This correction factor to the 1/4 power enters equation 8, modifying the value of $\gamma_f \beta_f$ in equation 8 by a factor ~ 2 . Pair annihilation significantly lowers the effect of pairs on the value of $\gamma_f \beta_f$ (see Pe'er & Waxman 2004).

Synchrotron emission affects several aspects of the calculation. First, the electron cooling time is shorter than the estimate of equation 1, which neglected synchrotron radiation. Second, the photon spectrum is different than the pure Compton spectrum calculated above, and depends on the details of the electron injection spectrum. Adopting the commonly used power law energy distribution of electrons injected above γ_m , one obtains a power law spectrum of synchrotron photons between photon energies $\varepsilon_{syn,min}$ and $\varepsilon_{syn,max}$. GRB observations suggest that if the low energy component is due to synchrotron emission, then $\varepsilon_{syn,min} \simeq 10^{-5} - 10^{-1} \times m_e c^2$, i.e., of

the same order as the assumed value of θ (Tavani 1996; Frontera *et al.* 2000). Assuming $A = u_{ph}/u_{el} \sim 1$, the photon density around $m_e c^2$ differs from the estimates above by factors \lesssim few, which enters equation 8 to the power 1/4. Finally, the synchrotron self-absorption would increase $\gamma_f \beta_f$, by an amount depending on spectral details. Numerical calculations for various models (Ghisellini *et al.* 1988; Pe'er & Waxman 2004; Pe'er *et al.* 2005) suggest that it does not change the $\gamma_f \beta_f$ of equation 8 by more than a factor of a few.

3. APPLICATION TO SUB-PHOTOSPHERIC DISSIPATION

As an application, we consider the effect of a photospheric term in the gamma-ray burst prompt emission (see Mészáros & Rees 2000; Rees & Mészáros 2004). Following Rees & Mészáros (2004) we assume that the dissipation occurs at $r > r_s \equiv \eta r_0$, where the observed photospheric luminosity is $L_\gamma(r) = L_0(r/r_s)^{-2/3}$. Here, L_0 is the total luminosity, $r_0 = \alpha r_g$ is the size at the base of the flow, r_s is the saturation radius where the bulk Lorentz factor asymptotes to η , r_g is the Schwarzschild radius of the central object, and $\alpha \geq 1$. For an internal shock model of GRB's, variations of the flow $\Delta\Gamma \sim \Gamma$ on a minimum time scale $\Delta t \sim r_0/c$ result in the development of shocks at a minimum radius $r_i \approx 2\Gamma r_s$, where $\Gamma \approx \eta$, thus $L_\gamma(r_i) = L_0(2\Gamma)^{-2/3}$. The comoving proton density is $n_p \approx L_0/4\pi r_i^2 c \Gamma^2 m_p c^2$, and the Thompson optical depth due to baryon related electrons at r_i is

$$\tau_{\gamma e} = \Gamma r_0 n_p \sigma_T = 100 L_{52} \Gamma_2^{-5} (\alpha m_1)^{-1}, \quad (13)$$

where $L_0 = 10^{52} L_{52} \text{ erg s}^{-1}$, $\Gamma = 10^2 \Gamma_2$, and $M \sim 10 m_1$ solar masses for the central object (e.g., black hole). Thus, for the parameters characterizing GRB's, the minimum shock dissipation radius can indeed be $r_i < r_{ph}$.

The normalized comoving temperature at r_i is

$$\begin{aligned} \theta &\equiv \frac{k_B T'}{m_e c^2} = \frac{k_B}{m_e c^2} \left(\frac{L_0}{4\pi r_s^2 \Gamma^2 c a} \right)^{1/4} (2\Gamma)^{-2/3} \\ &= 1.2 \times 10^{-3} L_{52}^{1/4} \Gamma_2^{-5/3} (\alpha m_1)^{-1/2}, \end{aligned} \quad (14)$$

where k_B , a are Boltzmann's and Stefan's constants. The shock waves (or generic dissipation mechanism) dissipate some fraction $\epsilon_d < 1$ of the kinetic energy, $L_k \sim L_0$, resulting in an internal (dissipated) energy density $u_{int} = L_0 \epsilon_d / 4\pi r_i^2 c \Gamma^2$. The electrons receive a fraction ϵ_e of this energy, so the ratio of the thermal photon energy density $u_{ph} = a T'^4$ to the electron energy density is

$$A \equiv \frac{u_{ph}}{u_{el}} = 0.44 \Gamma_2^{-2/3} \epsilon_{d,-1}^{-1} \epsilon_{e,-0.5}^{-1}, \quad (15)$$

where $\epsilon_d = 10^{-1} \epsilon_{d,-1}$ and $\epsilon_e = 10^{-0.5} \epsilon_{e,-0.5}$.

4. SPECTRUM AND EFFICIENCY

We calculated numerically the photon and particle energy distribution under the assumptions of §3 using the time dependent numerical model described in Pe'er & Waxman (2004b), including synchrotron emission and absorption, and with the addition of a thermal photospheric component (see Pe'er *et al.* 2005).

The self-consistent electron energy distribution is shown in figure 1 for three values of the dimensionless lower radius, $\alpha = 1, 10, 100$, i.e. scattering optical depths at the minimum dissipation radius of $\tau_{\gamma e} = 100, 10, 1$,

respectively (see eq. 13). The electrons accumulate at momentum values $\gamma_f \beta_f = 0.08, 0.10, 0.14$, in good agreement with the analytical calculations of §2. The small deviation (by $\lesssim 2$) between the values of equations 7, 8, and the numerical results originates from the synchrotron emission ($\epsilon_B = 10^{-0.5}$ in this graph). For completeness, we have added a curve showing the electron distribution in the absence of Compton scattering (i.e., with synchrotron emission and self absorption only). Synchrotron self absorption prevents the electrons from cooling below $\gamma\beta \approx 1$ (see also Ghisellini *et al.* 1988).

The observer-frame photon spectra for the three values of α (or optical depth) are shown in figure 2, for an assumed bulk Lorentz factor $\Gamma = 10^2$. At low optical depths, $\tau_{\gamma_e} = 1$, the thermal peak at $2.8\Gamma\theta/(1+z) \approx 10$ keV is prominent above the synchrotron emission component, which dominates the spectrum at low energies, 100 eV – 10 keV. Compton scattering produces the nearly flat spectrum at higher energies, 100 keV – 100 MeV.⁷ The small peaks at $\Gamma m_e c^2/(1+z) \approx 25$ MeV are due to pair annihilation. At $\tau_{\gamma_e} = 100$, Comptonization by electrons at $\gamma_f \beta_f$ produces the Wien peak at $\epsilon^{ob.} = \Gamma(\gamma_f \beta_f)^2 m_e c^2/(1+z) = 200$ keV, in accordance with the estimates of §2. Since most of the photons undergo multiple scattering, the Compton component at higher energies is significantly reduced. For an intermediate $\tau_{\gamma_e} = 10$, the peak is higher than $\Gamma\theta m_e c^2$ but lower than $\Gamma(\gamma_f \beta_f)^2 m_e c^2$, as expected.

In addition to the sub-photospheric internal shock cases, we have also calculated the spectrum in a “slow heating” scenario, for a high optical depth $\tau_{\gamma_e} = 100$ ($\alpha = 1$). In this scenario, the dissipated energy is continuously and equally distributed among the electrons in the dissipation region (Ghisellini & Celloti 1999; Pe’er & Waxman 2004). Unlike in previous calculations, here the electrons are assumed to be energized under a photosphere, so they interact with a strong thermal photon bath. Even though the details of the energy injection in this slow scenario are different from those of the internal shock scenario, the similar Compton energy balance considerations at the high optical depth $\tau_{\gamma_e} = 100$ result in a Wien peak at ~ 700 keV, similar to that of the internal shock scenario. This confirms the robustness of this result (see Pe’er *et al.* 2005, for details).

For a high optical depth in the dissipation region, the photons are trapped with the electrons in the plasma, before escaping at $\tau_{\gamma_e} \sim 1$. For an adiabatic expansion of the plasma following the internal shocks or dissipation occurring at $\tau_{\gamma_e} = 10 - 100$, Pe’er & Waxman (2004) showed that the photons lose 50% – 70% of their energy before escaping. This energy is converted into bulk motion of the expanding plasma. We thus expect the observed energy of the Compton peak, produced at sub-MeV, to be lowered by a factor of 2-3 from the values in figure 2, leading to an observed peak at $\approx 100 - 200$ keV. This result depends linearly on the unknown value of the Lorentz factor Γ above the saturation radius.

The accumulation of electrons at $\gamma_f \approx 1$ implies that most of the electron energy injected into the plasma is

⁷ Note that since the electrons distribution is affected by numerous physical processes, spectral curves which include both synchrotron and Compton cannot be fully decomposed into synchrotron and Compton components.

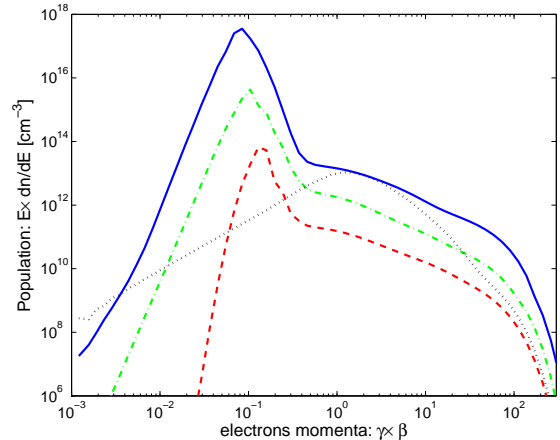


FIG. 1.— Electron distribution at the end of the dissipation. Results are for $L = 10^{52}$ ergs $^{-1}$, $\epsilon_e = \epsilon_B = 10^{-0.5}$, $\Gamma = 100$, $\epsilon_d = 0.1$, and internal shocks with $\alpha = 1$ (solid line), 10 (dot-dash), 100 (dash), and Thompson optical depths $\tau_{\gamma_e} = 100, 10, 1$, respectively. The dotted line shows the electrons momenta in the absence of Compton scattering, for $\alpha = 1$.

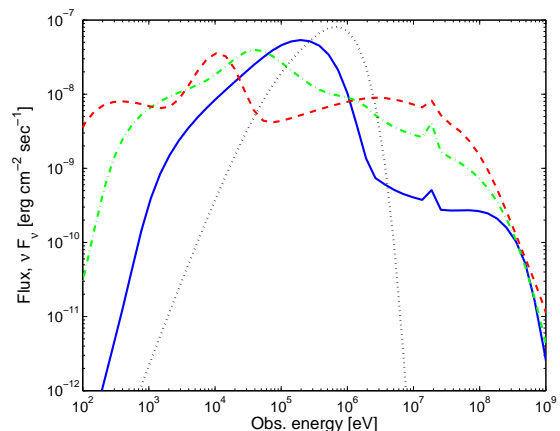


FIG. 2.— Time averaged spectra for the internal shock cases of figure 1 (solid, dash-dotted and dash-dash), and for the slow heating scenario (dots) with similar parameters as the solid curve. A redshift $z = 1$ in a flat universe with $\Omega_m = 0.3, \Omega_\Lambda = 0.7$, $H_0 = 70$ is assumed. The spectrum is not corrected for the energy loss due to adiabatic expansion following the dissipation, which lowers the energies by a factor 2-3.

transferred to photons during the dynamical time. For $\tau_{\gamma_e} \gtrsim 100$ at injection, most of this photon energy is near the peak, at an observed energy $\Gamma(\gamma_f \beta_f)^2 m_e c^2$. Since after adiabatic expansion the photons maintain $\sim 30\%$ of their energy, we conclude that in our model approximately 30% of the energy dissipated into electrons is ultimately converted into photons in the BATSE range.

5. SUMMARY AND DISCUSSION

We have considered a plasma composed of a low energy photon component and energetic particles, and showed that for Thompson optical depths $\tau_{\gamma_e} \gtrsim 1$ the electrons accumulate at $\gamma_f \beta_f \sim 0.1 - 0.3$, with only a weak dependence on the unknown parameter values. For $\tau_{\gamma_e} \approx 100$, the balance between Compton and inverse-Compton scattering by these electrons results in a spectral peak at $\sim 1 - 10$ keV in the plasma frame. We have presented a specific model for GRB prompt emission (§3) in which the dissipation occurs below the photosphere,

showing the applicability of this general result to GRB's.

For both an internal shock model or for a slow dissipation model in the presence of a photospheric component, we conclude that if a significant part of the energy is dissipated below the photosphere, the observed spectral peak clusters naturally in the BATSE range of hundreds of keV, for the inferred bulk Lorentz factors $\Gamma \sim 100$. This effect is further enhanced by pair creation, e.g. as considered in previous analyses (Pe'er & Waxman 2004; Rees & Mészáros 2004). Pairs will accumulate at the same $\gamma_f \beta_f$ as the electrons, forming a second photosphere at larger radius than the original baryon photosphere. Hence, if the dissipation process occurs below the second photosphere, similar results are obtained.

The results presented in §3 are largely independent of the specific model details. As shown in §4, numerical calculations including magnetic fields lead to results close to the analytical predictions. Similar results are obtained in §4 for both internal shocks or for a slow dissipation model, such as might be expected from magnetic dissipation. A similar spectral peak was also found in Pe'er & Waxman (2004), for an internal shock model with synchrotron and SSC emission but no thermal component. The dominant effect of a thermal component, as considered here for both internal shocks and slow dissipation, is to greatly increase the radiative efficiency, to

values $\sim 30\%$. We thus conclude that a Compton-inverse Compton balance leads to the creation of spectral peak at comoving photon energies 1 – 10 keV, which for inferred bulk Lorentz factors of order $\Gamma \sim 100\Gamma_2$ leads to observed peaks at 100 – 1000 Γ_2 keV, with a high efficiency. This is regardless of the nature of the dissipation process (shocks, magnetic reconnection, etc), provided it occurs at large optical depth, such as near or below the Thompson photosphere. If the spectral peak is a Wien peak, its observed energy is indicative of the asymptotic value of the bulk Lorentz factor Γ .

These results may be applicable to a range of compact objects, such as GRB's, XRF's possibly and blazars. XRF's show a clustering of the peak energy at ~ 25 keV, which may be attributed to the same mechanism, provided the characteristic Lorentz factor, or the optical depth, is somewhat smaller than assumed here. Our results may also apply to blazars, where a clustering of the peak energies at 1 – 5 MeV is reported (McNaron-Brown *et al.* 1995), if dissipation occurs at substantial optical depths and the bulk Lorentz factors are $\gtrsim 50$.

Research supported by NSF AST 0098416, 0307376, NASA NAFG5-13286.

REFERENCES

- Band, D., *et al.* 1993, ApJ, 413, 281
 Brainerd, J.J. 1998, in the 19th Texas Symposium on Relativistic Astrophysics and Cosmology, Eds.: J. Paul, T. Montmerle, and E. Aubourg (Paris: CEA Saclay)
 Crider, A., *et al.* 1997, ApJ, 479, L39
 Daigne, F. & Mochkovitch, R. 1998, MNRAS, 296, 275
 Frontera, F., *et al.* 2000, ApJS, 127, 59
 Ghirlanda, G., Celotti, A., & Ghisellini, G. 2003, A&A, 406, 879
 Ghisellini, G., & Celotti, A. 1999, ApJ, 511, L93
 Ghisellini, G., Guilbert, P.W., & Svensson, R. 1988, ApJ, 334, L5
 Guetta, D; Ghisellini, G; Lazzati, D; Celotti, A, 2004, A&A, 421, 877
 Guilbert, P.W., Fabian, A.C., & Rees, M.J. 1983, MNRAS, 205, 593
 Lazzati D, Ghisellini G, Celotti A & Rees MJ 2000, ApJ, 529, L17
 Lightman, A.P., & Zdziarski, A.A. 1987, ApJ, 319, 643
 McNaron-Brown, K., *et al.* 1995, ApJ, 451, 575
 Mészáros, P. 2002, ARA&A, 40, 137
 Mészáros, P, Ramirez-Ruiz, E, Rees, MJ, & Zhang, B 2002, ApJ, 578, 812
 Mészáros, P., & Rees, M.J. 2000, ApJ, 530, 292
 Pe'er, A., & Waxman, E. 2004, ApJ, 613, 448
 Pe'er, A., & Waxman, E. 2004, ApJ, in press (astro-ph/0409539)
 Pe'er, A., Mészáros, P., & Rees, M.J. 2005, in preparation
 Piran, T. 2004, Rev. Mod. Phys. 76, 1143
 Preece, R., *et al.* 1998, ApJ, 506, L23
 Preece, R., *et al.* 2000, ApJs.s., 126, 19
 Rees, M.J. & Mészáros, P., 2004, Ap.J. in press (astro-ph/0412702)
 Stern, B.E., & Poutanen, J. 2004, MNRAS, 352, L35
 Svensson, R. 1987, MNRAS, 227, 403
 Tavani, M. 1996, ApJ, 466, 768
 Waxman, E. 2003, Gamma-Ray Bursts: The Underlying Model, in Supernovae and Gamma-Ray bursters, Ed. K. Weiler (Springer), Lecture Notes in Physics 598, 393–418.